YU ISSN 0015—3206
FZKAAA 11 (2) 89 (1979)

CALCULATION OF THE RESPONSE FUNCTION AND EFFICIENCY OF A SMALL DETECTION SYSTEM FOR FAST NEUTRONS

B. EMAN

»Ruđer Bošković« Institute, Zagreb

and

N. STIPČIĆ—ŠOLIĆ

Bolnica »Braća dr Sobol«, Rijeka

Received 25 April 1979

UDC 539.1.074.88.01

Original scientific paper

The response function, efficiency and deposit energy spectra are calculated as functions of energy of incident neutrons and the geometry of the detection system. The thickness of the radiator and of the detector are taken into account. A comparison is made of deposit energy spectra of recoil protons for different energy spectra of incoming neutrons.

1. Introduction

The method for detecting fast neutrons, commonly used in neutron spectroscopy, is based on energy measurements or on energy-loss measurements of charged particles scattered from the target radiator. This, however, does not mean that all problems associated with the detection of fast neutrons are solved. The need for simple small-size detection systems appears in practice together with the need for more accurate measurements of the intensity and energy distribution of fast neutrons. Recent developments of detectors have made possible the construction of simple small-size detection systems[1]. Figure 1 shows the geometry of such

a system. A polyethylene foil or a deuterised polyethylene foil was placed in front of a Si detector of a surface area of a few mm^2, at a distance of a few millimeters from the detector. Since the Si crystal was thin, the deposit energy spectra were composed of contributions from energy losses of fast protons and from the total energy loss of low-energy protons stopped in the detector.

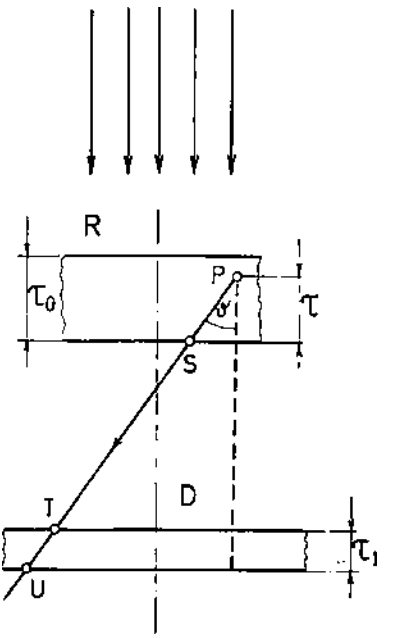

Fig. 1. Geometry of the detection system. A charged particle recoiled by a neutron at point P is passing through the radiator R and hits the detector D at the ponit T.

The aim of this paper is to calculate deposit-energy spectra as a function of the geometric parameters of the system and the energy distribution of incoming neutrons.

Previous calculations[2-6], performed by other authors, were based on the assumption that the detection system was axially symmetric and the beam of incoming neutrons monoenergetic. Calculations by Konijn[2] and Gotoh[3] were performed for a point neutron source and an infinitely thin radiator. The influence of the radiator thickness and of the energy dispersion of incoming neutrons were taken into account as a correction factor to the response function calculated previously[4]. Gotoh and Yagy[5] assumed that the beam of incoming neutrons is parallel to the axis of the system and that the energy loss of recoil protons in the radiator is negligible. Later on[6], however, they took into account the energy loss of protons in the radiator material.

In this paper we perform calculations of the response function and deposit energy spectra under the following assumptions: the detection system is considered to be axially symmetric; the beam of incoming neutrons is orthogonal to the radiator surface; the neutron beam is not monoenergetic; the energy loss of

recoil protons in the radiator is not negligible; protons are not all orthogonal to the surface of the detector; the single Si crystal is chosen to act as an E and dE/dx detector.

2. *Calculation of response functions*

The number of recoil protons impinging from the radiator upon the surface of the detector with energy between E_p and $E_p + \Delta E_p$ is usually called the response function.

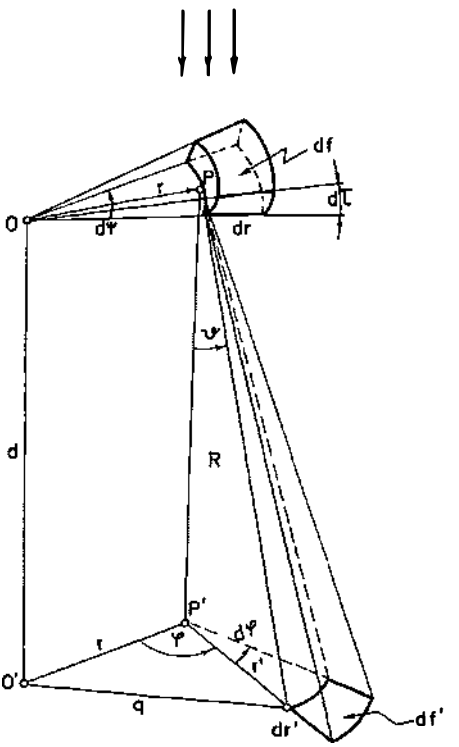

Fig. 2. The geometry and notation used in the calculations of the response functions of the system.

We denote by $n(E_n)$ the number of neutrons of energy between E_n and $E_n + \Delta E_n$, falling on a radiator surface of 1 cm^2. τ denotes the surface density in units of mg/cm^2. From $d\tau \cdot df$ milligrams of radiator material, neutrons with energy E_n will recoil protons with energy E_p at an angle $\Theta = \arccos(E_p/E_n)^{1/2}$. The number of protons with energy between E_p and $E_p + \Delta E_p$, emerging from the radiator surface df and falling on the detector surface df' (Fig. 2) is

$$\mathrm{n}(E_p)\,\mathrm{d}E_p = n(E_n)\,N\mathrm{d}\tau\mathrm{d}f\sigma(E_n, \Theta)\,\mathrm{d}\Omega. \tag{1}$$

Here N denotes the number of hydrogen atoms in 1 mg of radiator material, $\sigma(E_n, \Theta)$ is the differential cross section of elastically scattered neutrons in the laboratory system, $d\Omega$ is the solid angle subtended at the point P by the surface df'. Fig 2 shows that $d\Omega = df' \cos\Theta/R^2$, $R^2 = r'^2 + d^2$ and $r' = d \operatorname{tg}\Theta$. Inserting these expressions in Eq. (1) and integrating over the radiator of radius r_1 and over the detector surface of radius r_2, we obtain the total number of recoil protons:

$$\int n(E_p)\, dE_p = n(E_n)\, N \int \sigma(E_n, \Theta)\, r \sin\Theta\, d\tau\, dr\, d\Psi\, d\Phi\, d\Theta. \tag{2}$$

If $R(E)$ is the distance which a charged particle of energy E travels through the radiator material before being stopped, then the distance between two points, P and S, on the trajectory is equal to the difference of the range functions $R(E_P) - R(E_S)$. The proton at the point P, with energy $E_n \cos^2\Theta$ will travel a distance $\tau/\cos\Theta$ before leaving the radiator (Fig. 1). Thus,

$$R(E_n \cos^2\Theta) - R(E_p) = \tau/\cos\Theta, \tag{3}$$

where E_p is the energy of the recoil proton at the instant of its emergence from the radiator. Using Eq. (3), we can reduce the calculation of the response function to the following intergration:

$$n(E_p) = n(E_n)\, N \left(\frac{dR}{dE}\right)_{E=Ep} 2\pi \int \sigma(E_n, \Theta)\, r \sin\Theta \cos\Theta\, dr\, d\Theta\, d\Phi, \tag{4}$$

with the condition

$$\Phi = \arccos\left(\frac{r^2 + r'^2 - r_2^2}{2rr'}\right). \tag{5}$$

Let us denote by I the integration over r and Φ:

$$I = \int 2r\, dr\, d\Phi.$$

Then the relation (4) reduces to

$$n(E_p) = n(E_n)\, N\, 2\pi \left(\frac{dR}{dE}\right)_{E=Ep} \int_{\Theta_{min}}^{\Theta_{max}} \sigma(E_n, \Theta)\, I \sin\Theta \cos\Theta\, d\Theta. \tag{6}$$

The integral I takes the value $I(r) = r^2\pi$ if the relation between r, r' and r_2 allows the variable Φ to run from 0 to 2π. If the values of Φ are limited by Eq. (5), then the integral I is[7]

$$I(a, b) = \int_a^b 2 \arccos Z(r, r_2)\, r\, dr = \{r^2 \arccos Z(r, r_2) +$$

$$+ r_2^2 \arccos Z(r_2, r) - rr' [1 - Z(r, r_2)^2]^{1/2}\}_a^b, \tag{7}$$

$$Z(r, r_2) = \frac{r^2 + r'^2 - r_2^2}{2rr'}. \tag{8}$$

Since for a given r_1, r_2 and r' both parts of the integration over Φ, i.e. I(r) and I (a, b), will contribute to the integral I in Eq. (6), we have to calculate $I = I(a) + I(a, b)$ for a given set of parameters. For example, if $r_1 > r_2 + r$ and $r' < r_2$, then $I = I(r_2 - r') + I(r_2 - r', r_2 + r') = r_2^2 \pi$. There are only three different values for I. For $r_2 > r_1 + r'$ or $r_1 > r_2 + r'$, the integral I takes the simple form $r_1^2\pi$ or $r_2^2\pi$, respectively. In all other cases, $I = I(r_1, 0)$. Here $I(r_1, 0)$ denotes the right-hand side of Eq. (7) for $r = r_1$.

The upper limit of integration, Θ_{max}, is determined by the scattering angle, i.e. $\Theta_{max}^{(1)} = \arccos (E_p/E_n)^{1/2}$ for (n,p) scattering, or by the geometry of the detection system, $\Theta_{max}^{(2)} = \text{arctg}\,((r_1 + r_2)/d)$, if $\Theta_{max}^{(2)} < \Theta_{max}^{(1)}$. The lower limit Θ_{min} is zero if the difference in energy range, $R(E_n) - R(E_p)$, is smaller than the radiator thickness τ_0. If, however, the difference in energy range is larger, then Θ_{min} has to be calculated from Eq. (3).

To evaluate the response function, we make the following choice of the differential cross section $\sigma(E_n, \Theta)$ and the range functions $R(E)$:

A) A polyethylene radiator, $(CH_2)_n$

We choose

$$\sigma(E_n, \Theta) = (1 + 0.0025\, E_n + 0.00015\, E_n^2)\{3\,[1.206\, E_n +$$
$$+ (-1.86 + 0.0941\, E_n + 0.000130658\, E_n^2)^2]^{-1} +$$
$$+ [1.206\, E_n + (0.4233 + 0.13\, E_n)^2]^{-1}\} \cos\Theta. \tag{9}$$

This result is the same as that obtained by Gammel[8] for elastic (n, p) scattering multiplied by a correction factor[9]. In Eq. (9), the energy E_n is in MeV and the cross section in barns.

We write the range function for protons in the polyethylene foil in the form

$$R(E_p) = R_0 + R_1 E_p^{\alpha}, \tag{10}$$

and determine the parameters R_0, R_1 and α by the best fit to the tabulated values of range functions[10] (E_p is given in MeV). For protons of energies between 1 MeV and 14 MeV, with the set of paramteters

$$R_0 = 0.063\ \text{mg/cm}^2,\ R_1 = 1.936\ \text{mg/cm}^2 \text{ and } \alpha = 1.731,$$

the tabulated range function will be reproduced to within a deviation of less than 2%.

B) A deuterised polyethylene radiator, $(CD_2)_n$

To find a simple phenomenological form of the differential cross section for (n, d) elastic scattering, we made use of the fact that we need the differential cross sections only for angles smaller than $\pi/4$. We performed a multiparameter fit to experimental data for forward scattering, trying to reduce the number of parameters as much as possible. In this way, the simplest form of the response function we obtained describes experimental data for neutron energies between 0.5 MeV and 14 MeV reasonably well; this form of the differential cross section is

$$\sigma_d(E_n, \Theta) = 4 \cdot 10^A \cos\Theta, \tag{11}$$

where

$$A = C_1 - (C_2 E_n + C_3)\cos\Omega + (C_4 E_n + C_5)\cos^2\Omega \tag{12}$$

and $C_1 = 1.92093$, $C_2 = -0.30599$, $C_3 = 0.69661$, $C_4 = 0.27324$, $C_5 = -0.04158$, Ω is the scattering angle in the c.m. system. (E_n is in MeV and $\sigma_d(E_n, \Theta)$ in millibarns.)

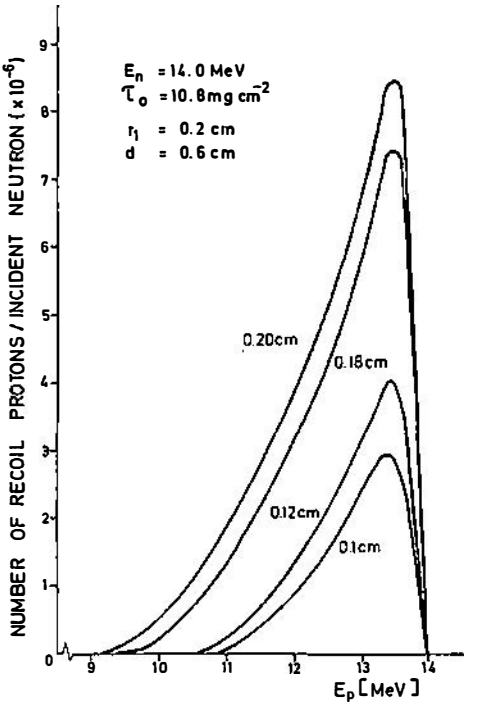

Fig. 3. The response functions for different radia of the detector. The energy of the incoming neutrons is 14 MeV, the thickness of the radiator $\tau_0 = 10.8$ mg.cm^2, the radius of the radiator $r_1 = 0.2$ cm and the radiator-detector distance $d = 0.6$ cm.

We have defined the agreement as »reasonably good« because the function A satisfies the condition

$$\sum_i \left(\frac{A_i - A_{exp}(i)}{\Delta A_{exp}(i)} \right)^2 < 1, \tag{13}$$

where $\Delta A_{exp}(i)$ denotes the error in the i-th piece of experimental data.

Thus, the agreement between the experimental[12] and calculated differential cross sections (Eq. (11)) is within the limits of experimental accuracy for neutron energies between 3.24 MeV and 20 MeV.

The range function for $(CD_2)_n$ radiators can be obtained from the range function for $(CH_2)_n$ radiators:

$$R(E) = 2R_0 + 2^{1-a} R_1 E^a. \tag{14}$$

However, to achieve better agreement with the tabulated values, the parameter a was increased to $a = 1.820$. In this way, the error in energy range was not larger than 2%. When the response function and efficiency are to be calculated for a deuterised radiator, expression (3) has to be properly modified.

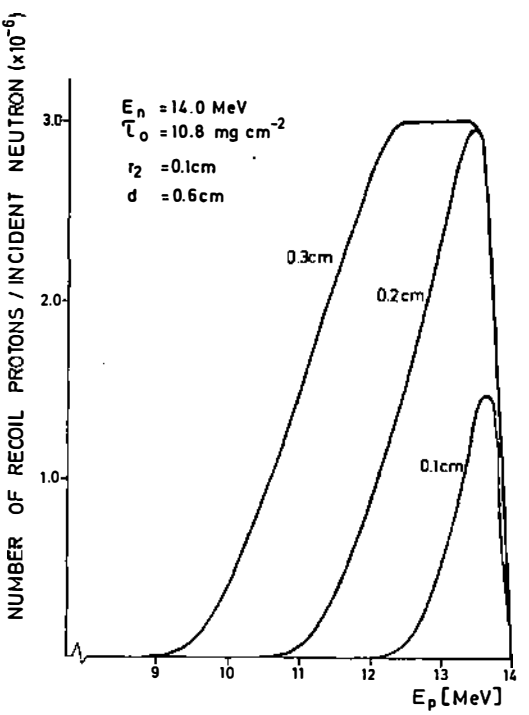

Fig. 4. The response function as a function of radiator radius.

The way of choosing the differential cross section and the range function for $(CH_2)_n$ and $(CD_2)_n$ radiators, described above, enabled us to investigate the behaviour of the response function for different geometrical parameters of the system. We required the system to have an efficiency larger than 10^{-6} for an incident flux of one neutron/cm^2, and the detector to have a surface not larger than a few mm^2. Figs. 3-6 show some of the results we obtained. In these figures we list the values of geometrical parameters of the detection system used in the calculation of the response functions and efficiency.

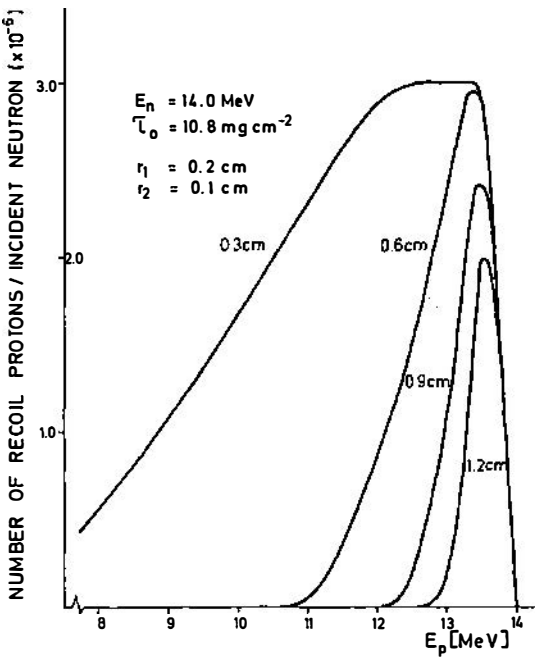

Fig. 5. The response function as a function of radiator-detector distance.

To test the calculations performed, we made use of the fact that for high-energy neutrons the efficiency does not depend on the thickness of the radiator τ_0. For n-p elastic scattering and an infinitely thin radiator, the efficiency of the system has a simple analytic form

$$\varepsilon_\infty = n(E_n) N\tau_0 \pi\sigma [B - (B^2 - 4r_1^2 r_2^2)^{1/2}], \tag{15}$$

where σ is the total cross section and $B = r_1^2 + r_2^2 + d^2$. Table 1 shows a comparison of the efficiency ε as a function of incident neutron energy for a radiator of a thickness of 10.8 mg/cm^2, and the corresponding value ε_∞ for an infinitely thin $(CH_2)_n$ radiator. The geometrical parameters are $r_1 = 0.2$ cm, $r_2 = 0.1$ cm and $d = 0.6$ cm.

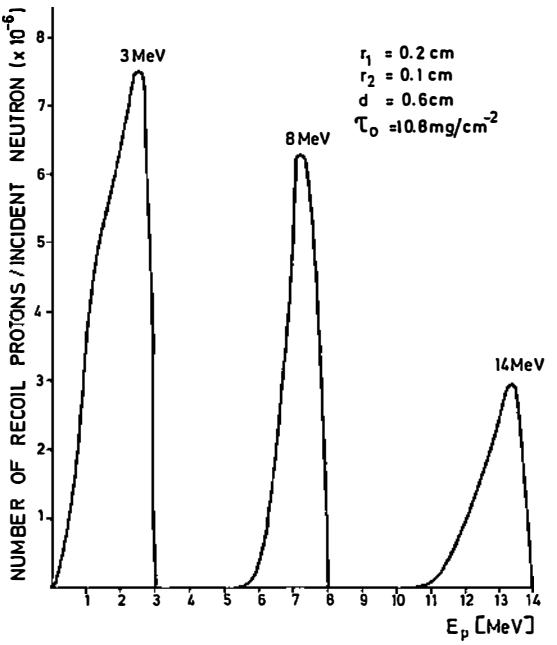

Fig. 6. The response functions for different energies of incoming neutrons.

TABLE 1

E_n (MeV)	1	2	3	4	6	10	13
ε ($\cdot 10^5$)	2.44	1.668	1.314	1.096	0.826	0.562	0.208
ε_∞ ($\cdot 10^5$)	0.348	0.816	1.276	1.095	0.829	0.559	0.207

Comparison of the efficiencies ε calculated by integration of Eq. (6) and those from Eq. (15).

3. Calculation of deposit-energy spectra of recoil particles for mono-energetic neutrons

We use a thin detector of a thickness of τ_1 mg/cm^2. The detector stops protons of low energy, while protons of energy higher than the limiting energy E_g will lose fraction of their energy in passing through the crystal. The deposit-energy spectrum to be detected by the system is obtained by the superposition of the part of the response function up to $E_p = E_g$ and the energy loss of protons with energy higher than E_g. The amout of energy loss in the detector depends on the energy of protons, E_p, and on the angle of incidence of protons falling on the surface of the Si detector.

The energy E of protons leaving the crystal can be determined from the diference between the possible energy range of protons $R(E_p)$ and the path they have traversed:

$$R(E) = R(E_p) - \frac{\tau_1}{\cos \Theta}. \tag{16}$$

However, because of the thickness of the radiator, protons of the same energy E_p will fall on the detector surface at different angles Θ. Eq. (16) has to be averaged over Θ:

$$R(E) = R(E_p) - \frac{\tau_1 \int_{\Theta_{min}}^{\Theta_{max}} f(\Theta) \cos^{-1} \Theta \, d\Theta}{\int_{\Theta_{min}}^{\Theta_{max}} f(\Theta) \, d\Theta}, \tag{17}$$

where $f(\Theta)$ is the angular distribution of protons of energy between E_p and $E_p + \Delta E_p$

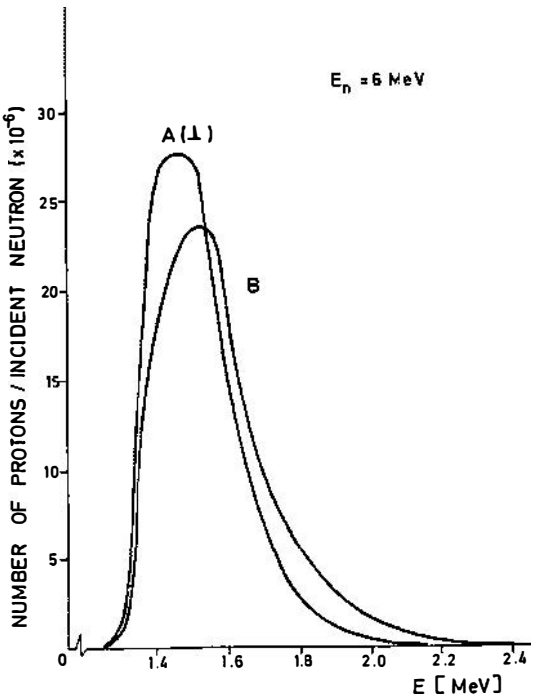

Fig. 7. Deposit energy proton spectra for neutrons of 6 MeV. Curve A was calculated assuming that all protons were orthogonal to the detector. Curve B was calculated using into account the incident angle of protons on the surface of the detector. $\tau_2 = 10.8$ mg,cm^2, $\tau_1 = 0.02329$ mg,cm^2.

The energy loss of protons in the passage through the detector is $\Delta E' = E_p - E$. The equidistant variation in energy of protons, ΔE_p, is not followed by the equidistant variation in energy loss, $\Delta E'$, so that the number of protons n (E') with energy loss between E' and $E' + \Delta E'$, is determined by the condition

$$\mathrm{n}\,(E')\,\Delta E' = \mathrm{n}\,(E_p)\,\Delta E_p. \tag{15}$$

In calculating the energy loss of protons and deuterons in the Si detector we used the tabulated values for range functions[13].

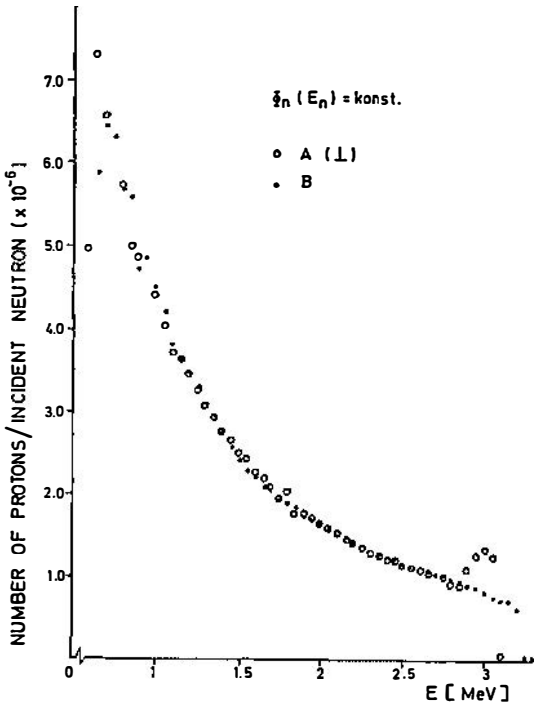

Fig. 8. Calculated deposit energy spectra for a continuous constant neutron spectrum in the range of 0-16 MeV. Open dots A denote that all recoil protons are orthogonal to the detector surface. Full dots B denote that the angle of incident protons is taken into account.

We assumed that the Si crystal was 0.02329 g/cm^2 thick, so that the limiting energy E_p was 3.14 MeV for protons and 4.16 MeV for deuterons. All other parameters of the detection system were the same as used previously, i.e. $r_1 = 0.2$ cm, $r_2 = 0.1$ cm, $d = 0.6$ cm and $\tau_0 = 10.8$ mg cm^{-2}.

Fig. 7 shows the calculated deposit energy spectra for an incoming neutron energy of 6 MeV. As can be seen, inclusion of the angle of incoming protons affects the shape of the spectrum, decreasing its maximum and producing a shift of the energy distribution resulting in larger energy losses.

4. *Continuous neutron spectra and discussion of the results*

To calculate the deposit energy spectrum of charged particles for a given energy spectrum of incoming neutrons, we calculated the response function for each energy interval ΔE_n of the normalised spectrum and then mapped the response function, described in section 3, onto the measuring range of the detector. We have shown that the influence of the angle of incoming charged particles on the detector surface is small except for the limiting-energy region where a small additional peak, appears, as shown in Fig. 8. Figure 8 shows the deposit energy spectra of protons for a neutron source of constant intensity in the range of 0—16 MeV. The geometrical parameters of the detector system are the same as those used in Fig. 7. The energy intervals $\Delta E_n = 0.1$ MeV and $\Delta E_p = 0.025$ MeV are sufficient to achieve a relative error per point of less than 1%.

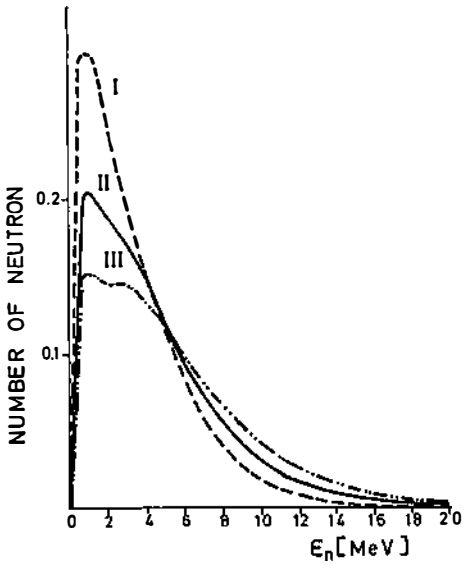

Fig. 9a. Energy spectra of different neutron sources.

Varying the incoming-neutron energy spectra varies the deposit energy spectra of recoil charged particles. Accordingly, variations are associated with the position and height of the maximum, as well as with the shape of the spectrum. Figs. 9a and 9b show that these variations are measurable; this further indicates that a detection system with a thin detector can be used to determine the energy distribution of incoming neutrons. We determined the energy distribution of incoming neutrons by using an iteration procedure based on the least-square fit to the deposit energy spectra measured.

The calculated deposit energy spectra and the efficiency of the detector can be compared with the spectra measured after the subtraction of the following effects[1,14]: multiple scattering in the radiator, contributions from reactions on carbon (e.g. $^{12}C(n, \alpha)$), detector-rim effect, and attenuation of neutrons in the target holder.

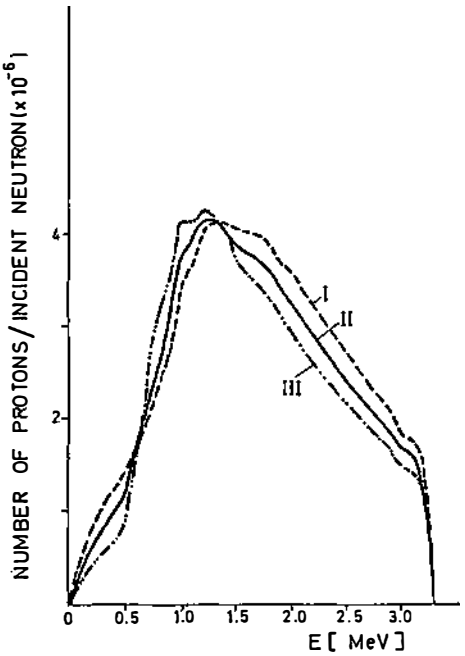

Fig. 9b. Deposit energy spectra of neutron sources shown in Fig. 9a.

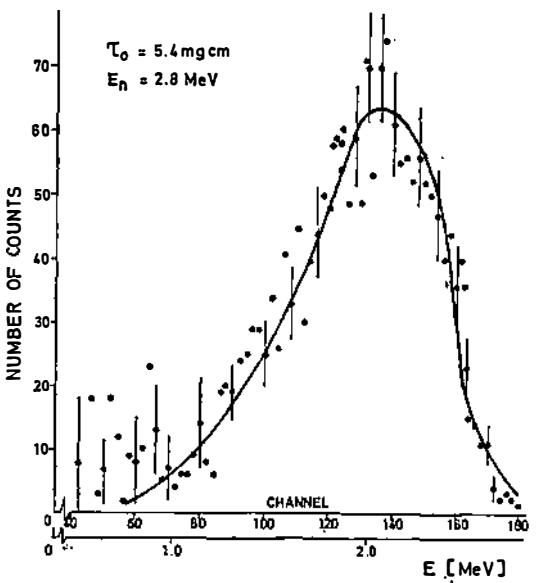

Fig. 10. Deposit energy proton spectra of neutrons of 2.8 MeV. The solid line represents the calculated spectra.

Fig. 10 shows that the measured spectra for monoenergetic incident neutrons are in good agreement with the calculated ones[1,14].

The spectrum of incident neutrons cannot be uniquely determined from a single measurement of deposit energy spectra. However, if the approximate position of the energy distribution maximum of incident neutrons is known, it is possible to determine the effective energy distribution of incident neutrons by varying the shape of the approximate spectrum and by comparing the corresponding calculated deposit energy spectra of recoil charged particles with the measured ones.

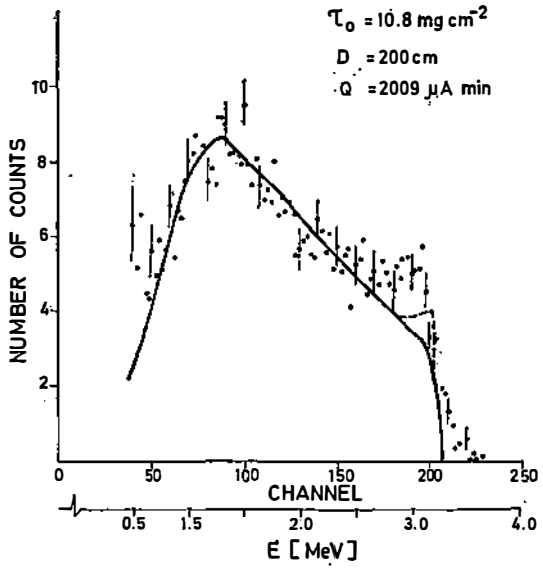

Fig. 11. Measured and calculated deposit energy proton spectra for continuous energy spectra of incident neutrons.

Fig. 11 shows a spectrum calculated in the manner described above. The dotted curve denotes the difference due to averaging over incident angle. The measurement was performed on the cyclotron of the »Ruđer Bošković« Institute in Zagreb[15]. In an ideal case, the energy spectrum of incoming neutrons can be determined from two measurements using different radiators[16] or different radiator thicknesses.

References

1) K. Kovačević, N. Stipčić, G. Paić, I. Šlaus, B. Eman, V. Pečar and M. Antić, Nucl. Instr. and Meth. **148** (1978) 291;
2) J. Konijn, A. Lauber and B. Tollander, AB Atomenergi Report AE-116 (1963);
3) H. Gotoh and H. Yagi, Nucl. Instr. and Meth. **101** (1972) 395;
4) V. K. Voitovetskii, I. L. Korsunskii and Yu. F. Pazhin, Nucl. Instr. and Meth. **33** (1965) 245;
5) H. Gotoh and H. Yagi, Nucl. Instr. Meth. **97** (1971) 419;
6) H. Gotoh, H. Yagi, and Y. Harayama, Nucl. Instr. and Meth. **109** (1973) 349;

7) I. S. Gradštein and I. M. Ryžik, Tablicy integralov, summ, rjadov i proizvedenij, Nauka, Moskva, 1971;
8) I. L. Gammel, Fast neutron physics, Wiley-Interscience, New York 1963;
9) E. L. Lomon and R. Wilson, Phys. Rev. **9C** (1974) 1329;
10) M. Rich and R. Madey, UCRL-2301 (1954), C. S. Zaidins, Nucl. Instr. and Meth. **120** (1974) 125;
11) N. O. Bazazyants, A. S. Zabrodskaya, A. F. Larina and M. N. Nikolaev, INDC (CCP)-107/L, IAEA, August 1978;
12) I. D. Seagrave, Evaluated summary of nucleon-deuteron elastic scattering data (1970);
13) C. Williamson, J. P. Boujot and I. Picard, CEA-3042, Saclay 1966;
14) N. Stipčić-Šolić, Ph. D. thesis, Zagreb 1978;
15) N. Stipčić-Šolić, I. Šlaus, G. Paić, B. Antolković and B. Eman, to be published;
16) N. Stipčić, I. Šlaus, G. Paić and B. Eman, Nucl. Instr. and Meth. **164** (1979) 525.

RAČUNANJE FUNKCIJE ODZIVA I EFIKASNOSTI MALOG DETEKTORSKOG SISTEMA ZA BRZE NEUTRONE

B. EMAN

Institut »Ruđer Bošković«, Zagreb

i

N. STIPČIĆ-ŠOLIĆ

Bolnica »Braća dr Sobol«, Rijeka

UDK 539.1.074.88.01

Originalni naučni rad

Pretpostavlja se samo da je detekcioni sistem aksijalno simetričan i da neutroni upadaju okomito na površinu radijatora. Kao radijator služi polietilenska ili deuterizirana polietilenska folija. Kao E i dE/dx detektor služi tanki silicijev detektor površine nekoliko mm^2. Izračunate su funkcije odziva, efikasnosti i deponiranog spektra u ovisnosti o energiji upadnih neutrona, debljini radijatora, debljini detektora te geometrijskim parametrima sistema. Uspoređuju se izračunati deponirani spektri za različite energetske raspodjele upadnih neutrona.